Computer Methods and Programs in Biomedicine 200 (2021) 105832

Contents lists available at ScienceDirect

Computer Methods and Programs in Biomedicine

journal homepage: www.elsevier.com/locate/cmpb

A model based on cellular automata to estimate the social isolation impact on COVID-19 spreading in Brazil

P.H.T. Schimit

Informatics and Knowledge Management Graduate Program Universidade Nove de Julho Rua Vergueiro, 235/249 São Paulo, CEP: 05001-001, SP, Brazil

ARTICLE INFO

Article history:
Received 2 June 2020
Accepted 4 November 2020

Keywords:
COVID-19
probabilistic cellular automata
SARS-CoV-2
SEIR model
social isolation model

ABSTRACT

Background and objective

Many countries around the world experienced a high increase in the number of COVID-19 cases after a few weeks of the first case, and along with it, excessive pressure on the healthcare systems. While medicines, drugs, and vaccines against the COVID-19 are being developed, social isolation has become the most used method for controlling the virus spreading. With the social isolation, authorities aimed to slow down the spreading, avoiding saturation of the healthcare system, and allowing that all critical COVID-19 cases could be appropriately treated.

By tuning the proposed model to fit Brazil's initial COVID-19 data, the objectives of the paper are to analyze the impact of the social isolation features on the population dynamics; simulate the number of deaths due to COVID-19 and due to the lack of healthcare infrastructure; study combinations of the features for the healthcare system does not collapse; and analyze healthcare system responses for the crisis.

Methods

In this paper, a Susceptible-Exposed-Infected-Removed model is described in terms of probabilistic cellular automata and ordinary differential equations for the transmission of COVID-19, flexible enough for simulating different scenarios of social isolation according to the following features: the start day for the social isolation after the first death, the period for the social isolation campaign, and the percentage of the population committed to the campaign.

Results

Results showed that efforts in the social isolation campaign must be concentrated both on the isolation percentage and campaign duration to delay the healthcare system failure. For the hospital situation in Brazil at the beginning of the pandemic outbreak, a rate of 200 purchases per day of intensive care units and mechanical ventilators is the minimum rate to prevent the collapse of the healthcare system.

Conclusions

By using the model for different scenarios, it is possible to estimate the impact of social isolation campaign adhesion. For instance, if the social isolation percentage increased from 40% to 50% in Brazil, the purchase rate of 150 intensive care units and mechanical ventilators per day would be enough to prevent the healthcare system to collapse. Moreover, results showed that a premature relaxation of the social isolation campaign can lead to subsequent waves of contamination.

1. Introduction

The ongoing pandemic of Coronavirus Disease-2019 (COVID-19), caused by the virus SARS-CoV-2 (Severe Acute Respiratory Syndrome - Coronavirus 2), was first identified in Wuhan, China, in December 2019. As of October 6th, 2020, more than 35.3 million cases have been reported, resulting in more than 1.03 million deaths [9,55]. There are a few points that may explain the magnitude of the problems caused by COVID-19: the first is the fast spread of the SARS-CoV-2 virus [24,40,47]; the second is the wide

E-mail address: schimit@uni9.pro.br

https://doi.org/10.1016/j.cmpb.2020.105832
0169-2607/

range of symptoms, with some cases presenting no symptoms, and others presenting fever and severe respiratory problems [60], complicating health advice at the onset of symptoms, for instance [40]; and the third is the colossal number of cases requiring medical treatment at the same time, collapsing many healthcare systems around the globe [15,48,51].

Governments, scientists, and specialists have proposed protocols for dealing with the situation, like washing hands carefully, a proper sneezing and coughing etiquette, self-isolation, social distancing, quarantine, and complete lockdown [19]. Due to the rapid escalation of cases, countries quickly moved to the lockdown to stop the COVID-19 spreading [48,51]. The term lockdown has been used for describing different scenarios, but it means the "banning of any non-essential public gatherings, closure of educational and public/cultural institutions, ordering people to stay home apart from exercise and essential tasks" [15]. Therefore, according to the level of decreased social contact, a term has been used. Here, we will consider different levels of social isolation, which starts on self-isolation, until a lockdown. However, in order to use a quantity of isolation, we will refer to any isolation by social isolation, and the percentage is the decreased level of social contact.

Regarding what we know so far about COVID-19, Susceptible-Exposed-Infected-Removed (SEIR) models have been used for predictions and analysis [19–21,28,53,61]. In this model, susceptible individuals become exposed when contacting infected, and after an incubation period, exposed individuals become infected. When infected, individuals may die due to the disease or get cured, changing to removed. For the exposed stage (E_I), researchers are dealing with uncertainties regarding the start of the disease. Some studies show that the incubation period for COVID-19 is 4-5 days [15,25], there are cases of transmission during incubation [62], and evidence of an early peak of SARS-CoV-2 replication (day 5) than SARS (days 7-10) [54]. One issue related to regular SEIR models is the absence of the asymptomatic state, and the use of one single infected state for hospitalized, non-hospitalized, and hospitalized in Intensive Care Units (UCI).

Cellular automata have been used for investigating the spread of contagious diseases, and some of the advantages are the flexibility of local rules and configuration of state transitions [59]. Instead of using deterministic state transitions, the Probabilistic Cellular Automata (PCA) is more suitable for epidemiological studies [1,2,45]. Accordingly, it has been used for studying migratory movements on the persistence of contagious disease [5,16], the impact of the time delay in the spreading of a disease based on SEIR model [44], the adaptation of cellular automata for using real population density maps [18], and disease infection in groups of individuals [37]. Also, for large homogeneous and well-mixed populations, Ordinary Differential Equations (ODE) can be interpreted as a mean-field approximation of the PCA model [4,32,42].

Therefore, here we propose a model based on Probabilistic Cellular Automata and Ordinary Differential Equations, where the states are: Susceptible (S), Exposed (E_I), Infected Symptomatic (I_S), Infected Asymptomatic (I_A), Infected non-hospitalized (I_{S1}), Infected hospitalized (I_{S2}), Infected in ICU (I_{S3}), and Recovered/Removed (R). A S-individual, when exposed to E_I, I_A, I_S, I_{S1}, I_{S2}, and I_{S3} states (not necessarily all and at the same time), has a probability of being infected, changing the state to E_I. For E_I-individuals, after a period of incubation, may either change to symptomatic (I_S) or asymptomatic (I_A). For I_A-individuals, there is a probability of getting recovered, becoming R. After a period of symptoms, an I_S-individual has a probability of not needing hospital, being an I_{S1}-individual, and an I_{S1}-individual has a probability of getting recovered, becoming R. If an I_S needs a hospital, the state is updated to I_{S2} (which has its own probabilities of cure and death), and if a hospitalized case needs an ICU or mechanical ventilator, the state is updated to I_{S3} (also, with its own probabilities of cure and death). All individuals may die due to other causes, with a S-individual replacing them, to keep the total number of individuals constant.

It is important to emphasize that the main idea in proposing a model with eight states and fifteen parameters (to be presented) is to make the model flexible and easy to input data considering the COVID-19 uncertainties. Also, COVID-19 requires different approaches for the infected state due to different outcomes for the disease case-by-case. Other works also consider parameters for externalities of the epidemiological model (such as the parameters to be presented here which are related to the healthcare system dynamic) [3,28,39,61].

By using available data of COVID-19, and considering the Brazilian situation on hospital beds, ICUs and mechanical ventilator at the beginning of pandemic outbreak, we propose a SEIR model adjusted to the disease requirements. The objective of this paper is to explore social isolation features such as the start of the social isolation campaign, the percentage of reduced contacts and the duration of the campaign on the spread of the COVID-19. Also, we will explore continuous and periodic isolation operations in order to understand the dynamics of the disease and the impact on the health system for a medium to long-range period.

The paper is organized as follows: the next section contains the proposed SEIR model based on PCA and ODE approaches; the third section has the results of the simulations, and in the fourth section, the results are discussed.

2. Methods

The PCA model consists of a lattice with side n and a total size of $n \times n = N$ cells with periodic boundary conditions (forming a toroidal surface to eliminate edge effects), where each cell represents an individual in one of the eight states: S, E_i, I_A, I_S, I_{S1}, I_{S2}, I_{S3}, or R. Cellular automata models usually rely on local interactions to represent an infectious process, and here we expand the neighbourhood, as presented on [42], where, at the beginning of each time step, individuals make C connections to neighbours inside a Moore radius r. Therefore, the probability of connection between an individual centred on a square of side $2r+1$, and another individual at layer i is given by $q_{i,r} = 2(r+1-i)/r(r+1)$. The layer is composed by the $8l$ cells at the border of the square of side $2l+1$, with $l \leq r$. For example, if $r = 4$, the probability of interacting to one cell of layers 1, 2, 3, and 4 are $q_{1,4} = 0.4$, $q_{2,4} = 0.3$, $q_{3,4} = 0.2$, and $q_{4,4} = 0.1$, respectively, and after randomly choosing the layer, a random cell of the layer is also randomly chosen. The random contact network formed by these connections may have a "high" clustering coefficient and "small" average shortest path length, characteristics of social networks [42].

Consider the example shown in Fig. 1 with $r = 4$. The first layer $i = 1$ is blue, the second layer $i = 2$ is grey, the third layer $i = 3$ is red, and the fourth layer $i = 4$ is yellow. The white cells are examples of $C = 5$ connections for a maximum radius of $r = 4$. After randomly picking up the layer according to $q_{i,r}$, a random cell in that layer is randomly chosen.

Due to COVID-19 uncertainties, parameters used for the states transitions are either based on probabilities, or periods before changing the state. Therefore, at each time step a S-individual may be infected with probability $P_i(\nu_i) = 1 - e^{-k\nu_i}$, where ν_i is based on the number of connections with different types of infective individuals, given by $\nu_i = 0.5\nu_{E_I} + \nu_{I_A} + 2\nu_{I_S} + 0.5\nu_{I_{S1}} + 0.5\nu_{I_{S2}} + 0.5\nu_{I_{S3}}$, where ν_{E_I} is the number of E_I-individuals, ν_{I_A} is the number of I_A-individuals, and so on for other states, and k is a parameter related to the disease infectivity. The weights are related to the infectiousness at each stage of the COVID-19, with symptomatic (I_S) individuals being twice as infective as asymptomatic (I_A), and advanced stages (I_{IS1}, I_{IS2}, and I_{IS3}) with half the

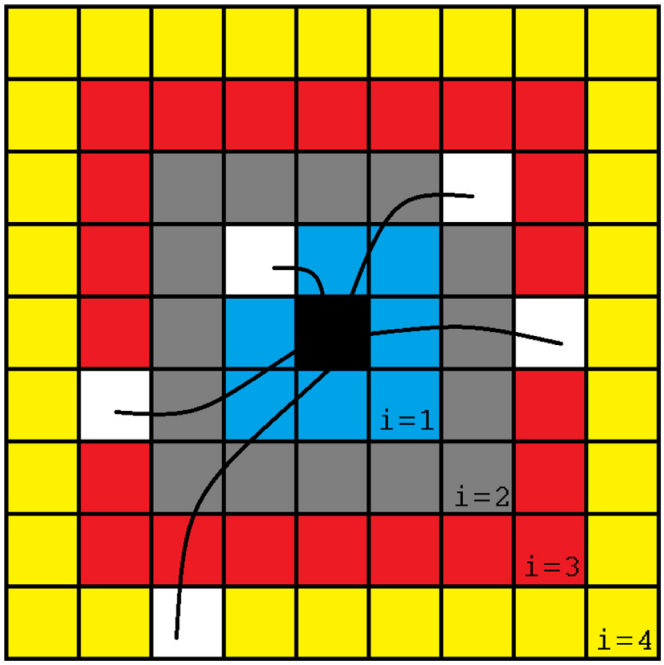

Fig. 1. Neighbourhood example with four layers ($r = 4$) and five connections ($C = 5$).

infectiousness of I_S due to limited contact with their close relatives and health care personnel. Although states I_{IS2} and I_{IS3} are related to individuals at hospitals beds and ICUs, they are responsible for spreading the disease due to health care overwhelmed situation [8,56]. We consider a lower infectivity for E_I-individuals due to conclusion about the infectiousness starting 12 hours before the onset of symptoms for symptomatic, and 4.6 days when asymptomatic [15]. Also, there are some cases of infection from a recent exposed individual [62]. Therefore, E_I-individuals are mildly infective for a period T_{E_I}.

After the T_{E_I} period, P_{I_S} is the probability of the E_I individual becomes symptomatic I_S, and $1 - P_{I_S}$ to become asymptomatic. When asymptomatic, I_A-individuals have an average period of T_{I_A} days of infectivity, and after this period, they become recovered (R-individual). For I_S-individuals, there is an average delay period of T_{I_S} days before going to their final stages of the disease. After this period, a fraction P_{hosp} needs hospitalization, going to I_{S2} state, and $1 - P_{hosp}$ becomes I_{S1}. An I_{S1}-individual has an average period of T_{CIS1} days for recovering from the disease. For I_{S2}-individuals, the average period for a hospital stay is T_{HIS_2}, and after this period, either I_{S2}-individual is transferred for an ICU with probability P_{ICU}, die with probability P_d, or get cured. Finally, I_{S3}-individuals have an average hospital stay of T_{HIS_3} days, and after this period, there is a probability P_{d-IS3} of dying due to disease complications and $1 - P_{d-IS3}$ of getting cured. Finally, all individuals may die due to natural causes with probability P_n per time step.

Therefore, one time step consists of generating C connections per individual; for S-individuals, the transition $S \to E$ is tested according to $P_i(v_i)$; for the other states the transitions are tested conforming to the respective periods and probabilities; and, after all individuals calculations, their states are updated synchronously at the end of the time step.

An approach for the PCA model can be described in terms of the following ODE if we consider that individuals are homogeneously distributed over space:

$$\begin{aligned}
\frac{dS(t)}{dt} &= -aS(t)(E_I(t) + I_S(t) + I_A(t) + I_{S1}(t) + \\
&\quad + I_{S2}(t) + I_{S3}(t)) + d_{S2}I_{S2}(t) + \\
&\quad + d_{S3}I_{S3}(t) + e(E_I(t) + I_S(t) + I_A(t) + \\
&\quad + I_{S1}(t) + I_{S2}(t) + I_{S3}(t) + R(t)) \\
\frac{dE_I(t)}{dt} &= aS(t)(E_I(t) + I_S(t) + I_A(t) + I_{S1}(t) + \\
&\quad + I_{S2}(t) + I_{S3}(t)) - \alpha_S E_I(t) - \alpha_A E_I(t) + \\
&\quad - eE_I(t) \\
\frac{dI_S(t)}{dt} &= \alpha_S E_I(t) - \beta_{S1} I_S(t) - \beta_{S2} I_S(t) - eI_S(t) \\
\frac{dI_A(t)}{dt} &= \alpha_A E_I(t) - b_A I_A(t) - eI_A(t) \\
\frac{dI_{S1}(t)}{dt} &= \beta_{S1} I_S(t) - b_{S1} I_{S1}(t) - eI_{S1}(t) \\
\frac{dI_{S2}(t)}{dt} &= \beta_{S2} I_S(t) - b_{S2} I_{S2}(t) - \beta_{S3} I_{S2}(t) + \\
&\quad - d_{S2} I_{S2}(t) - eI_{S2}(t) \\
\frac{dI_{S3}(t)}{dt} &= \beta_{S3} I_{S2}(t) - b_{S3} I_{S3}(t) + \\
&\quad - d_{S3} I_{S3}(t) - eI_{S1}(t) \\
\frac{dR(t)}{dt} &= b_A I_A(t) + b_{S1} I_{S1(t)} + b_{S2} I_{S2}(t) + \\
&\quad + b_{S3} I_{S3}(t) - eR(t)
\end{aligned} \tag{1}$$

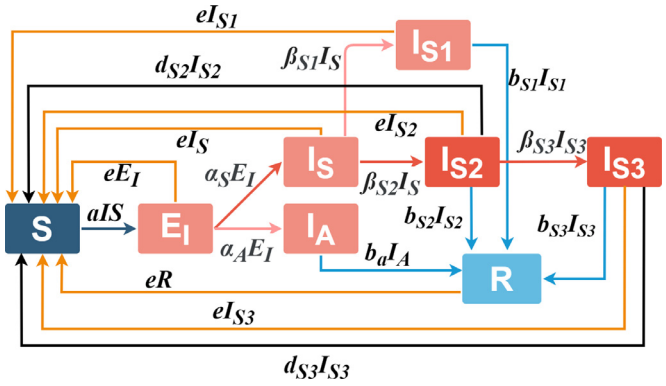

Fig. 2. States transitions for the SEIR model.

where a is the infection rate constant; b_a, b_{S1}, b_{S2}, and b_{S3} are the recovering rate constant for I_A, I_{S1}, I_{S2}, and I_{S3} individuals, respectively; d_{S2} and d_{S3} are the death rate constant due to disease for I_{S2} and I_{S3} individuals; e is the death rate constant due to other causes; α_A and α_S are the symptomatic and asymptomatic constant rates from exposed individuals; and β_{S1}, β_{S2}, and β_{S3} are constant rates for symptomatic individuals related to non-hospitalization, hospitalization and hospitalized cases requiring ICUs for I_S, I_{S1}, and I_{S2}, respectively. Fig. 2 contains the diagram of the transitions with the associated variables.

Note that $dS(t)/dt + dE_I(t)/dt + dI_S(t)/dt + dI_A(t)/dt + dI_{S1}(t)/dt + dI_{S2}(t)/dt + dI_{S3}(t)/dt + dR(t)/dt = 0$, therefore the total number of individuals is constant, and $S(t) + E_I(t) + I_S(t) + I_A(t) + I_{S1}(t) + I_{S2}(t) + I_{S3}(t) + R(t) = N$. We assume that for the period analyzed, the number of deaths is equal to the number of births.

The basic reproduction number (R_0) can be derived from the ODE by using the Next-Generation Matrix (NGM), which is an alternative for models with finite categories of individuals. Therefore, we decompose the Jacobian matrix from the system of ODEs as $T + \Sigma$, where T is the transmission part, containing the production of new infected, and Σ is the transition part, containing changes in the states [11], only for the infected states. With these matrices, we calculate the dominant eigenvalue (spectral radius) ρ of the matrix $-T\Sigma^{-1}$. For the ODE (1), at the infection-free steady

state with $E_I = I_S = I_A = I_{S1} = I_{S2} = I_{S3} = 0$, we have:

$$T = \begin{bmatrix} a & a & a & a & a & a \\ 0 & 0 & 0 & 0 & 0 & 0 \\ 0 & 0 & 0 & 0 & 0 & 0 \\ 0 & 0 & 0 & 0 & 0 & 0 \\ 0 & 0 & 0 & 0 & 0 & 0 \\ 0 & 0 & 0 & 0 & 0 & 0 \end{bmatrix} \text{ and}$$

$$\Sigma = \begin{bmatrix} -\alpha_S - \alpha_A - e & 0 & 0 & 0 & 0 & 0 \\ \alpha_S & -\beta_{S1} - \beta_{S2} - e & 0 & 0 & 0 & 0 \\ \alpha_A & 0 & -b_A - e & 0 & 0 & 0 \\ 0 & \beta_{S1} & 0 & -b_{S1} - e & 0 & 0 \\ 0 & \beta_{S2} & 0 & 0 & -b_{S2} - \beta_{S3} - d_{S2} - e & 0 \\ 0 & 0 & 0 & 0 & \beta_{S3} & -b_{S3} - d_{S3} - e \end{bmatrix}$$

Then, the spectral radius $\rho(-T\Sigma^{-1})$ returns:

$$R_0 = \frac{a}{\nu_1} + \frac{a\alpha_A}{\nu_1\nu_2} + \frac{a\alpha_S}{\nu_1\nu_3} + \frac{a\alpha_S\beta_{S2}}{\nu_1\nu_3\nu_4} + \frac{a\alpha_S\beta_{S1}}{\nu_1\nu_3\nu_5} + \frac{a\alpha_S\beta_{S2}\beta_{S3}}{\nu_1\nu_3\nu_4\nu_6} \quad (2)$$

with:

$$\begin{aligned} \nu_1 &= \alpha_A + \alpha_S + e \\ \nu_2 &= b_A + e \\ \nu_3 &= \beta_{S1} + \beta_{S2} + e \\ \nu_4 &= \beta_{S3} + b_{S2} + d_{S2} + e \\ \nu_5 &= b_{S1} + e \\ \nu_6 &= b_{S3} + d_{S3} + e \end{aligned}$$

Here, we will consider the effective basic reproduction number, R_t, which is similar to R_0 by assuming that susceptibility is not complete in the population, and can be used for a partially recovered population. It is given by:

$$R_t(t) = S(t)R_0 \quad (3)$$

where S(t) is the normalized concentration of susceptible individual at time step t in the population.

The constant parameters from Equation (1) can be obtained from PCA simulation, since the ODE is a mean-field for the PCA model [42]. Therefore,

$$\begin{aligned} a &\simeq \frac{\Delta E_I(t)_{S\to E_I}}{S(t)\Gamma(t)\Delta t} \\ \alpha_S &\simeq \frac{\Delta I_S(t)_{E_I\to I_S}}{E_I(t)\Delta t} \\ \alpha_A &\simeq \frac{\Delta I_A(t)_{E_I\to I_A}}{E_I(t)\Delta t} \\ b_A &\simeq \frac{\Delta R(t)_{I_A\to R}}{I_A(t)\Delta t} \\ \beta_{S1} &\simeq \frac{\Delta I_{S1}(t)_{I_S\to I_{S1}}}{I_S(t)\Delta t} \\ \beta_{S2} &\simeq \frac{\Delta I_{S2}(t)_{I_S\to I_{S2}}}{I_S(t)\Delta t} \\ \beta_{S3} &\simeq \frac{\Delta I_{S3}(t)_{I_{S2}\to I_{S3}}}{I_{S2}(t)\Delta t} \\ d_{S2} &\simeq \frac{\Delta S(t)_{I_{S2}\to S}}{I_{S2}(t)\Delta t} \\ d_{S3} &\simeq \frac{\Delta S(t)_{I_{S3}\to S}}{I_{S3}(t)\Delta t} \\ e &\simeq \frac{\Delta S(t)_{I_S\to S} + \Delta S(t)_{I_A\to S} + \Delta S(t)_{I_{S1}\to S}}{(S(t)+\Gamma(t)+R(t))\Delta t} + \\ &\quad + \frac{\Delta I_{S2}(t)_{I_S\to S} + \Delta S(t)_{I_3\to S} + \Delta S(t)_{R\to S}}{(S(t)+\Gamma(t)+R(t))\Delta t} + \\ &\quad + \frac{\Delta S(t)_{S\to S}}{(S(t)+\Gamma(t)+R(t))\Delta t} \end{aligned} \quad (4)$$

where $\Gamma(t) = E_I(t) + I_S(t) + I_A(t) + I_{S1}(t) + I_{S2}(t) + I_{S3}(t)$; $\Delta E_I(t)_{S\to E_I}$ is the increase per time step of exposed individuals due to contamination process; $\Delta I_S(t)_{E_I\to I_S}$ is the increase per time step of symptomatic from exposed individuals; $\Delta I_S(t)_{E_I\to I_A}$ is the increase per time step of asymptomatic from exposed individuals; $\Delta I_{S1}(t)_{I_S\to I_{S1}}$ is the increase per time step of non-hospitalized from symptomatic individuals; $\Delta I_{S1}(t)_{I_S\to I_{S2}}$ is the increase per time step of hospitalized from symptomatic individuals; $\Delta I_{S1}(t)_{I_S\to I_{S1}}$ is the increase per time step of ICU patients from hospitalized individuals; $\Delta S(t)_{I_{S2}\to S}$ is the increase per time step of susceptible individuals due to the death caused by the disease of hospitalized individuals; $\Delta S(t)_{I_{S3}\to S}$ is the increase per time step of susceptible individuals due to the death caused by the disease of ICU patients. Finally, $\Delta S(t)_{E_I\to S}$, $\Delta S(t)_{I_S\to S}$, $\Delta S(t)_{I_A\to S}$, $\Delta S(t)_{I_{S1}\to S}$, $\Delta I_{S2}(t)_{I_S\to S}$, $\Delta S(t)_{I_3\to S}$, $\Delta S(t)_{R\to S}$ are the increase per time step of susceptible individuals due to the death for other causes of exposed, symptomatic, asymptomatic, non-hospitalized, hospitalized, and ICU patients, respectively.

In the next sections, the results are presented.

3. Results

In this section, we present the results of the simulations with the proposed model. The results are divided into five situations, starting with a comparison between the PCA and ODE approaches, followed by a simulation of the model using real data from Brazil without social distancing control and hospital beds and UCIs unlimited. Then, an analysis of the social isolation features contrasting with the condition with absolutely no isolation between individuals is presented. The fourth situation is an investigation of the minimum percentage of isolation in the population in order to the healthcare system can deal with the ill individuals who require hospital beds, ICUs and mechanical ventilators. Finally, the periodic characteristics of the social isolation campaigns and individuals perceptions of the disease are explored.

3.1. Comparison of PCA and ODE approaches

In order to have the PCA lattice with a similar size of Brazilian population, we consider $n = 14500$, and $N = 210,250,000$ (the Brazilian population is around 211,000,000 inhabitants according to IBGE [36], Brazilian Institute of Geography and Statistics, in direct translation). The movements characteristics are $C = 32$ and $r = 8$. The parameters for PCA simulations are: $T_{E_i} = 5$ days, $P_{I_S} = 0.5$, $P_{I_A} = 1 - P_{I_S} = 0.5$, $T_{I_S} = 4$ days, $T_{I_A} = 14$, $P_{hosp} = 0.2$, $T_{CIS1} = 14$ days, $T_{HIS_2} = 8$ days, $P_{ICU} = 0.33$, $P_d = 0.0165$, $T_{HIS_3} = 10$ days, $P_{d-IS3} = 0.5$, and $P_n = 0.1$. The initial conditions will always be $S(0) = N - 10$, $E_I(0) = 10$, and $I_S(0) = I_A(0) = I_{S1}(0) = I_{S2}(0) = I_{S3} = 0$ with individuals randomly distributed over space. The simulation runs for $t_s = 3000$ time steps (one time step is considered to be one

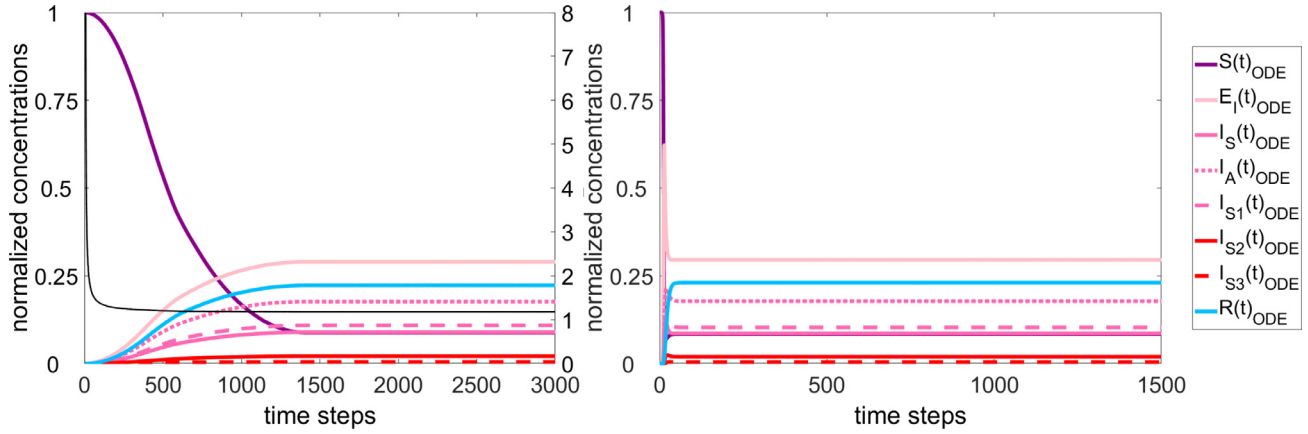

(a) PCA simulation. (b) ODE simulation.

Fig. 3. Temporal evolution of PCA and ODE approaches.

day). The ODE parameters are calculated from the PCA average results of the last 10 time steps by using Eqs. 4, and we obtain: $a = 7.2 \times 10^{-9} \times N$, $\alpha_S = 0.1$, $\alpha_A = 0.1$, $b_A = 0.0714$, $\beta_{S1} = 0.2$, $\beta_{S2} = 0.05$, $\beta_{S3} = 0.0412$, $d_{S2} = 0.002$, $d_{S3} = 0.05$, and $e = 0.0948$. The ODE is numerically solved with the 4$^{\text{th}}$-order Runge-Kutta method with integration time step of 0.01. The initial conditions for ODE are $S(0) = (N - 10)/N$, $E_I(0) = 10/N$, and $I_S(0) = I_A(0) = I_{S1}(0) = I_{S2}(0) = I_{S3} = 0$.

Fig. 3 shows the temporal evolution of PCA (Fig. 3a) and ODE (Fig. 3b) simulations. For the PCA simulation, the effective basic reproduction number (R_t) is also plotted. Note the good agreement between the two approaches when we compare the steady states of the simulation (where the ODE parameters are based on PCA simulation). The initial transient is not similar as a result of data from the permanent regime of PCA being used to simulate the ODE, and ODE being a mean-field approach for PCA. Other combinations of parameters have also been tested showing similar results.

3.2. Simulation of Brazil

Concerning the COVID-19 parameters, we will use the following data: an average period of $T_{E_i} = 5$ days [15] for E_I-individuals, probabilities of $P_{I_S} = 0.5$, and $P_{I_A} = 1 - P_{I_S} = 0.5$ [15,52] for an E_I-individual becoming symptomatic or asymptomatic, respectively. Once in one of these states, the average period is $T_{I_S} = 4$ days [15] for symptomatic, and $T_{I_A} = 14$ days [15,40] for asymptomatic. Symptomatic individuals soon need hospital, and they are probably the most tested individuals. Therefore, $T_{I_S} < T_{I_A}$, because after this period either I_S-individuals need a hospital with probability $P_{hosp} = 0.2$ [27] becoming a I_{S2}-individual, or they are considered a non-hospitalized case, becoming an I_{S1}-individual.

I_{S1}-individual remains in this state for an average period of $T_{CIS1} = 14$ days [7], and then it is cured (R-individual). A hospitalized I_{S2}-individual stays at the hospital bed for an average period of $T_{HIS_2} = 8$ days [15]. After this period, either there is a probability of $P_{ICU} = 0.33$ [8] to require an ICU treatment, or die due to disease with probability $P_d = 0.0165$ [26], or get cured (R-individual). Finally, an ICU patient remains in intensive care for an average period of $T_{HIS_3} = 10$ days [15] with a mortality of $P_{d-IS3} = 0.5$ [15] after this period (or $1 - P_{d-IS3} = 0.5$ of getting cured). All individuals may die due to other causes with probability $P_n = 0.000036$ [50] (considering the data from Brazilian population).

The last parameter for the model is k, related to the infectivity of the disease. This parameter will be tuned by using COVID-19 accumulated deaths for the first twenty-five days of the outbreak in Brazil after the first known death, which happened in March 6$^{\text{th}}$, 2020. In this period, there is no, if any, effect of initial isolation actions (which started somehow at March 21$^{\text{th}}$, 2020). This parameter has been adjusted manually by considering the accumulated number of death in the period from March 6$^{\text{th}}$, 2020 to March 30$^{\text{th}}$, 2020 [31]. Note in Fig. 4 that the adjustment with $k = 0.15$ is conservative when comparing with real data [31]. Table 1 contains a summary of all variables and values considered here.

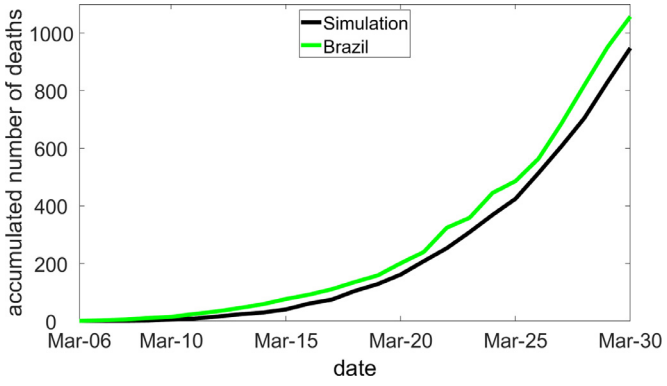

Fig. 4. The accumulated number of deaths for the first twenty-five days after the first death in Brazil. Simulation and Brazilian official data.

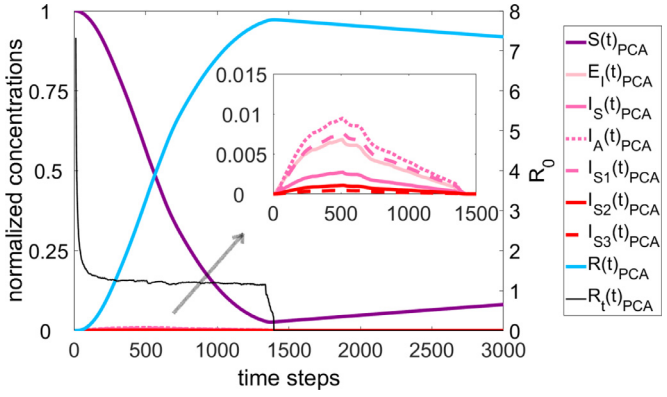

Fig. 5. Temporal evolution of COVID-19 in Brazil without restrictions of hospital and ICU beds.

Table 1
Model parameters

Param.	*Description*	*Value*	*Unit*	*Source*
k	Related to disease infectivity.	0.150	-	estimated
T_{E_I}	Average period of incubation.	5	days	[15]
P_{I_S}	Probability of an Exposed becoming Infected Symptomatic.	0.5	-	[15,52]
P_{I_A}	Probability of an Exposed becoming Infected Asymptomatic.	0.5	-	[15,52]
T_{I_A}	Average period of infectiousness for I_A.	14	days	[15,52]
T_{I_S}	Average period for state I_S.	4	days	[15]
P_{hosp}	Probability of a I_S case becoming hospitalized (I_{S2}).	0.2	-	[27]
P_{ICU}	Probability of a hospitalized case (I_{S2}) requires a ICU (I_{S3}).	0.33	-	[8]
T_{CIS1}	Average period of cure for I_{S1}.	31	days	[7]
T_{HIS2}	Average period of I_{S2} in the hospital.	8	days	[15]
T_{HIS3}	Average period of I_{S3} in the hospital.	10	days	[15]
P_d	Average probability of death due to COVID-19.	0.0165	-	[26]
P_{d-IS3}	Probability of death for I_{S3}.	0.5	-	[15]
P_{c-IS3}	Probability of cure for I_{S3}.	0.5	-	[15]
P_n	Probability of death due to natural/other causes.	0.000036	-	[50]

By using these values, the PCA simulation is shown in Fig. 5 for the initial conditions. It is worth noting that the model used here does not consider limits of hospital and ICU/mechanical ventilators beds. Therefore, at the peak of the hospital and ICU beds demand, it would be required 228,243 hospital beds and 93,692 ICU/mechanical ventilators. The total number of deaths until the fade-out of any type of infected individuals in the population is 3,887,423. Also, after the initial peak of infections with $R_t \approx 7$, the effective basic reproduction number remains constant with $R_t \approx 1.2$ while the disease is active. These values of R_t have been computed by using Eqs. 2, 3, and 4.

However, Brazil is far from offering 100,000 ICU/mechanical ventilators for this crisis. Data acquired at the beginning of the pandemic showed that there were around 426,380 hospital beds, 55,100 ICU beds, and 10311 mechanical ventilators available in Brazil [6,38]. Although the recommended occupation rate of ICU beds in Brazil is 85% [49], usually the rate is higher than 90%. Therefore, by considering that the medical staff can handle the ICU and mechanical ventilators management during this period, we consider that I_{S3} may require either ICU or mechanical ventilator. Also, by considering an occupation rate of 80% on hospital beds, 85% on ICU beds, and 50% on mechanical ventilators, there will be available to COVID-19 patients a total of 85,276 hospital beds and 13,421 ICU/mechanical ventilators. From here, we will refer to the management of ICU and mechanical ventilators only by ICU. Therefore, these limits on patients treatment are set on the model on the state transitions $I_S \to I_{S2}$, when symptomatic individuals require a hospital, and $I_{S2} \to I_{S3}$, when hospitalized individuals require an ICU. We consider that if there are beds available, the transition is done; otherwise, the individual dies. In this case, transitions $I_S \to S$ and $I_{S2} \to I_S$ are counted. In this restriction of hospital and ICU beds situation, there would be a total of 13,591,960 deaths, with 2,051,427 deaths due to ICU limit, and 11,540,533 due to hospital beds limit. Fig. 6 shows the temporal evolution for this situation.

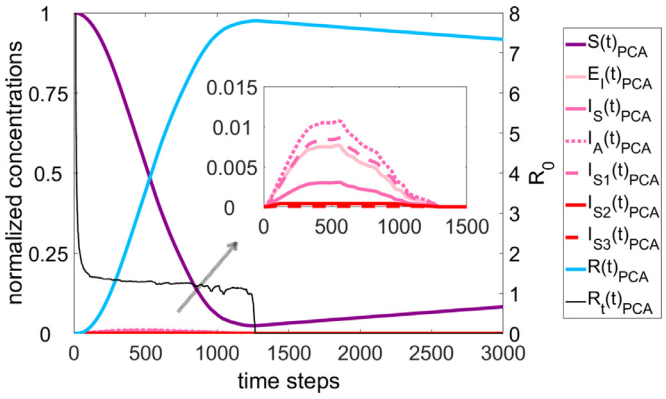

Fig. 6. Temporal evolution of COVID-19 in Brazil with restrictions of hospital and ICU beds.

3.3. Social isolation effects

The social isolation is modelled by considering three parameters: the beginning of the social isolation after the first confirmed death (Q_S), the duration of the social isolation (Q_P), and the percentage of social contact reduction (Q_ϕ). By using these three features of a social isolation campaign, it is possible to understand their effects on the number of deaths due to healthcare system collapse and the time for the healthcare system to collapse.

Therefore, the same simulation configuration presented in the previous section to generate Fig. 6 is used here with the following modifications: After Q_S time steps of the first death, the social isolation campaign begins. During the campaign, individuals cut a percentage Q_ϕ of the C contacts per time step. Thus, if $C = 32$ and $Q_\phi = 0.25$, individuals have an average of 24 contacts per time step. The isolation campaign is active for Q_P time steps. One simulation is run for each combination of the following values: $Q_S = 0, 5, 10, 15, 20, 25$, $Q_\phi = 0.2, 0.3, \ldots 1$, and $Q_P = 1, 2, \ldots 12$, resulting in 648 cases. If the first death occurs in time step t_d, each simulation runs for $t_d + Q_S + 180$ time steps. In this period, the system does not achieve a permanent regime, but it is enough for making some considerations.

The first data to be analysed is the number of days for the healthcare system to collapse, when the deaths due to limits of hospital and ICU beds start to happen. This result is shown in Fig. 7, where the number of days for the healthcare system to collapse is plotted in function of the duration of social isolation (Q_P, in weeks) and the isolation percentage (Q_ϕ), for the six values of the isolation campaign start (Q_S). The figure colour is related to the gradient $g(x, y)$ of the surface $f(x, y)$, given by $g(x, y) = \sqrt{(\delta f/\delta x)^2 + (\delta f/\delta y)^2}$.

Note that there are only small shifts between the surfaces of different values of Q_S. Also, the gradient of the figure is useful to check that combining the efforts on Q_P and Q_ϕ is a better option than invest only on either the period or percentage of social isolation. Thus, the isolation campaign should start with at least $Q_P \gtrsim 6$ and $Q_\phi \gtrsim 0.6$.

A second analysis consists of the saved lives in function of the social isolation parameters. By considering the same simulations of the previous analysis, the number of saved lives when comparing with simulation without any social isolation (Fig. 6) is shown in Fig. 8. The period used for comparison is the 180 days follow-

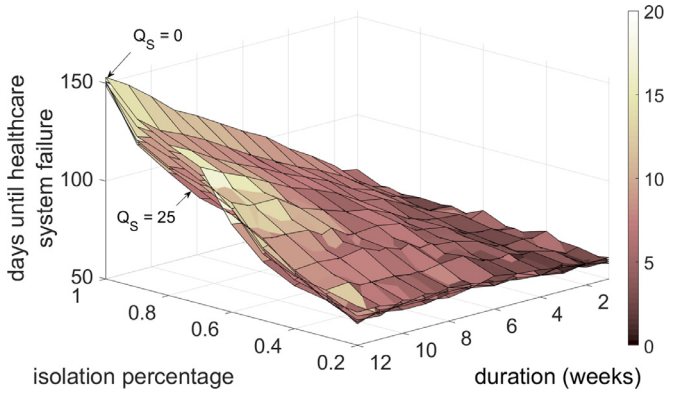

Fig. 7. Number of days for the healthcare system to collapse in function of the duration of social isolation (Q_P, in weeks) and the isolation percentage (Q_ϕ), for the six values of the isolation campaign start (Q_S). The colour and the colour bar are related to the gradient of the plot.

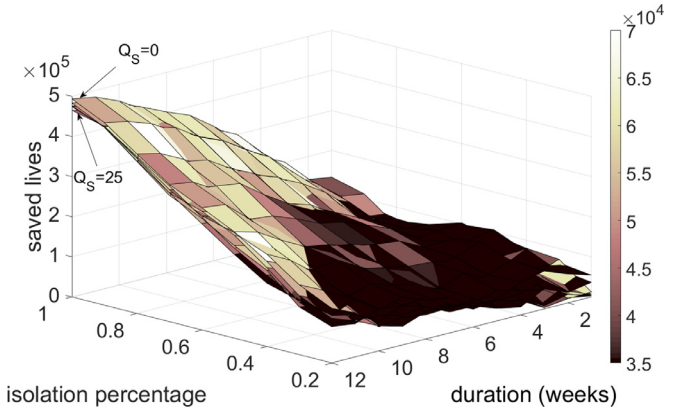

Fig. 8. Saved lives in function of the duration of social isolation (Q_P, in weeks) and the isolation percentage (Q_ϕ), for the six values of the isolation campaign start (Q_S). The colour and the colour bar are related to the gradient of the surface.

ing the beginning of social isolation campaign. The deaths difference due to unavailable hospital and ICU beds is plotted in function of Q_P (in weeks), and Q_ϕ, for the six values of Q_S. The colour of the figure is related to the gradient of the surface. As in the previous analysis, the isolation campaign should start with at least $Q_P \gtrsim 6$ and $Q_\phi \gtrsim 0.6$, considering that any extra effort from this point could have more significant gains than increasing efforts on low values of Q_P and Q_ϕ.

In this section, the number of hospital and ICU beds, and mechanical ventilator were fixed during the whole simulation. Of course, once the COVID-19 outbreak takes place, government and healthcare association act to increase these numbers. Also, for the cases simulated here, independent of the social isolation features, the COVID-19 is not entirely eliminated of the population. All results showed that the COVID-19 returns to rapidly spread once the social isolation campaign is down. These points are better explored in the next sub-sections and in the supplementary file.

3.4. Healthcare system response to the crisis

One of the primary responses of healthcare systems around the globe to the pandemics crisis is the purchase of ICU and mechanical ventilators due to the high increase of the demand. Therefore, the minimum daily purchase rate of ICU beds to the healthcare system does not collapse is investigated. We consider a constant daily purchase rate (τ) during a simulation from the beginning of social isolation campaign (Q_S), and the minimum rate is taken. The Fig. 9 contain the results of the simulations for $Q_S =$

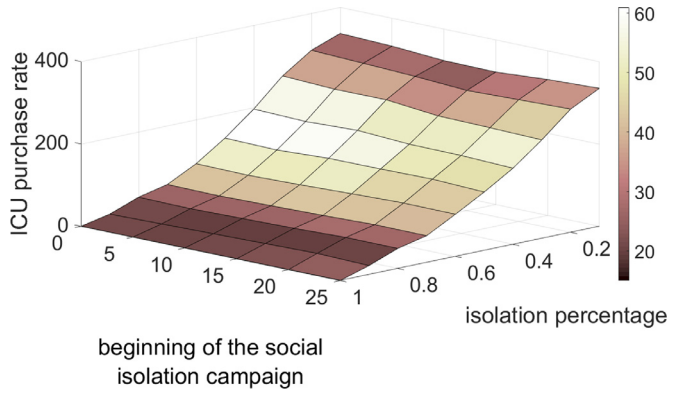

Fig. 9. Minimum constant daily purchase rate of ICU beds in function of the isolation percentage (Q_ϕ) and the isolation campaign beginning (Q_S). The colour and the colour bar are related to the gradient of the surface.

$0, 5, 10, 15, 25$, and $Q_\phi = 0.2, 0.3, \ldots 1$, with the colour of the figure representing the surface gradient (same process of Figs. 7 and 8). For each combination of these parameters, simulations are run for $\tau = 0, 5, 10, \ldots 400$, and the simulation with the minimum value of τ where no deaths occurred due to hospital and ICU beds collapse is considered for the figure. Each simulation runs for Q_S + 365 time steps, and the social isolation campaign is active during the rest of the simulation.

Note that the beginning of the campaign does not influence the ICU purchase rate. On the other hand, an increase in the social isolation from $Q_\phi = 0.4$ to $Q_\phi = 0.6$ may reduce the daily constant purchase rate of ICU by around 100 unities.

A supplementary file is provided with different formats of social isolation campaigns and their effects on the time evolution of the disease.

4. Discussion

The objective of this paper was not to propose a breakthrough model which would change the current analysis of COVID-19 whose results should be strictly taken into consideration for public authorities. The objective was to propose a model based on reliable models used for past epidemics to analyse how social isolation can interfere with the COVID-19 dynamics. We used initial data from Brazil, but the same model could be used for any territory or country. It is clear that if the whole population is confined at home, the disease slows down. However, it is not clear that this is the only variable to consider for decisions concerning the COVID-19 future. As discussed in [22], numerous mathematical models have been suggested since the beginning of the pandemic, and many of them have limitations (usually with an optimistic view) for forecasting the COVID-19 spreading with precision. Not to mention the uncertainty regarding the SARS-Cov-2 or the disease statistics, for instance.

What mathematical models can do is to bring light on COVID-19 issues. Here, we attempted to cover how the social isolation features may change the disease dynamics. Therefore, by proposing a model based on probabilistic cellular automata and ordinary differential equations for a modified Susceptible-Exposed-Infected-Removed case, we added the social isolation variables, as the beginning and the period of the campaign, and the percentage of social contact reduction, for evaluating the impact on the population dynamics. The healthcare system has also been considered, by classifying the infected individuals according to the disease stage and adding healthcare infrastructure data, like hospital beds, intensive care units, and mechanical ventilator numbers.

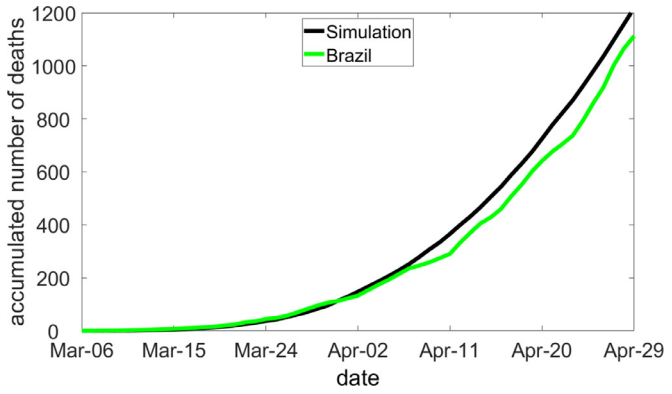

Fig. 10. Accumulated number of deaths for the first 55 days after the first death in Brazil. Data from simulation and Brazilian official data.

Cellular automata have been used for studying many diseases, such as dengue [10,34], Chagas disease [46], foot and mouth disease in feral pigs [12], bubonic plague [23], and hepatitis B [57], with some of these models considering some heterogeneities in the spatial distributions of the population. Also, in [41], ordinary differential equations were a good approach for heterogeneous population models based on a wide range of complex random networks. Here, probabilistic cellular automata with a randomly varying neighbourhood could replicate the first days of the COVID-19 spreading. Fig. 10 contains the expansion of the data presented in Fig. 4 (that is, the simulation runs without social isolation), and the divergent trend is visible few days after some social distancing procedures, which started in March 24th, 2020 (also using data from [31]).

It is worth mentioning that the flexibility for implementing a model in cellular automata has its drawback. In a regular PC with a 4GHz processor with 16 GB RAM, the simulations of this paper would take two months to be completed. Some efforts have been made to run the model in a Graphics Processing Unit (GPU), which reduced the time to one week and a half.

The first result of the paper is the model itself. Although not usual, the classification of infected states according to the infection stage, with the representation of each stage by a state in the model may help to describe the COVID-19 specification fully. In a study for the Italian case [17], the infected state has also been split into five states: infected, diagnosed, ailing, recognized and threatened, similar to the states E, I_A, I_S, I_{S1}, I_{S2}, and I_{S3} presented here. The comparison between the PCA and ODE models showed a good agreement between the approaches.

The second result helps to understand the impact of the social isolation on the Brazilian healthcare system, and it was presented in Fig. 7. The number of days for the healthcare system to collapse was shown in terms of the isolation percentage and the duration of the campaign. For a short period of social isolation with a low percentage of reduced contacts, the system would collapse in 50 days after the first registered death. The company *Inloco*, which estimates the social isolation level based on cell phones location data from networks providers [29], showed that this estimation is around 40% since March, 24th, 2020.

The estimative was that the hospital and ICU beds will be full in around 80 days after the first death. Since the first registered death occurred in March, 6th, 2020, the prediction of the paper would be May 25th, 2020. The peak of hospitals crisis was around June, extending to early August, depending on the region. The long-term results presented here reduced the importance of the day when the isolation campaign starts. Of course that in a short-term, the evolution of infected states is delayed, as also reported in [60].

Certainly, there would be responses from the Brazilian healthcare system. Therefore, we simulated the minimum purchase rate of intensive care units to consider all patients that could require such treatment. Considering the social isolation features in Brazil for the beginning of the pandemic outbreak, the rate was around 200 ICUs/day ($Q_\phi = 0.4$ and $Q_S = 18$) according to Fig. 9. Also, a small increase in social isolation percentage to $Q_\phi = 0.5$ would reduce the rate to around 150 ICUs/day. It is hard to estimate the exact number of ICU and mechanical ventilators purchased for the healthcare system in Brazil, but a data from Brazilian Ministry Of Health updated in April, 20th, 2020, showed that 14,100 mechanical ventilators had been purchased, to be fully available for use in July 20th, 2020. Considering the beginning of the social isolation (in some states) as of March 24th, 2020, the average purchase rate per day is around 120. This number does not consider private healthcare or purchases made directly by states.

Finally, some social isolation campaign configurations were presented in the supplementary file. The conclusion is that if we consider one data from the epidemic evolution or one data from the healthcare system for the decision about starting and stopping a campaign, there will be a long disease persistence in the population, with oscillations of the infected states over time.Such oscillatory behaviour for public health issues has also been found in a vaccination campaign, for instance [43]. Further waves of COVID-19 propagation have been concerned specialists due to premature relaxation of social isolation campaigns worldwide [58]. Furthermore, campaigns that hardly slow the virus propagation make the disease endemic in population for many years.

Overall, delaying the SARS-Cov-2 spreading seems to be the most effective way to avoid the healthcare system to collapse and save lives. There are some variables to delay the spreading, and here we attempted to investigate some of them. Splitting the campaign decisions into different variables may help to deal with some side effects of social distancing, as reduced sleep quality of self-isolated individuals [56], extreme social isolation of people living with HIV [30] or living in long-term care facilities [13], for instance. The next steps of this work could be in the following directions: use a population density map to build the spatial cellular automata; consider a network of cities, to study how the disease spread over the country, and; consider groups of individuals [14,33,35,37] as an approach for the social contact.

4.1. Statements of ethical approval

Ethics approval was not required for this study.

4.2. Funding

PHTS is supported by grants #307194/2019-1 and #402874/2016-1 of Conselho Nacional deDesenvolvimento Científico e Tecnológico (CNPq) and grant #2017/12671-8, São Paulo Research Foundation (FAPESP)

Declaration of Competing Interest

The author declares that there are no conflicts of interest regarding the publication of this paper.

Supplementary material

Supplementary material associated with this article can be found, in the online version, at 10.1016/j.cmpb.2020.105832

References

[1] E. Ahmed, H. Agiza, On modeling epidemics. including latency, incubation and variable susceptibility, Phys. A 253 (1998) 347–352.

[2] E. Ahmed, H. Agiza, S. Hassan, On modeling hepatitis b transmission using cellular automata, J. Stat. Phys 92 (1998) 707–712.
[3] J.P. Arcede, R.L. Caga-Anan, C.Q. Mentuda, Y. Mammeri, Accounting for symptomatic and asymptomatic in a SEIR-type model of COVID-19, Mathematical Modelling of Natural Phenomena 15 (2020), doi:10.1051/mmnp/2020021.
[4] L. Berec, Techniques of spatially explicit individual-based models: Construction, simulation, and mean-field analysis, Ecological Modelling 150 (1-2) (2002) 55–81, doi:10.1016/S0304-3800(01)00463-X.
[5] A. Bouaine, M. Rachik, Modeling the impact of immigration and climatic conditions on the epidemic spreading based on cellular automata approach, Ecological Informatics 46 (May) (2018) 36–44, doi:10.1016/j.ecoinf.2018.05.004.
[6] B.S. de Carvalho, L.F.C. Silva, H. Matarazzo, B. Zoca, N. Melo, Cenário dos hospitais no brasil. 2019Retrieved from https://fbh.com.br/wp-content/uploads/2019/05/CenarioDosHospitaisNoBrasil2019_10maio2019_web.pdf Accessed: 15.04.20.
[7] K.S. Cheung, I.F. Hung, P.P. Chan, K. Lung, E. Tso, R. Liu, Y. Ng, M.Y. Chu, T.W. Chung, A.R. Tam, C.C. Yip, K.-H. Leung, A. Yim-Fong Fung, R.R. Zhang, Y. Lin, H.M. Cheng, A.J. Zhang, K.K. To, K.-H. Chan, K.-Y. Yuen, W.K. Leung, Gastrointestinal Manifestations of SARS-CoV-2 Infection and Virus Load in Fecal Samples from the Hong Kong Cohort and Systematic Review and Meta-analysis, Gastroenterology (2020), doi:10.1053/j.gastro.2020.03.065.
[8] J. Chu, N. Yang, Y. Wei, H. Yue, F. Zhang, J. Zhao, L. He, G. Sheng, P. Chen, G. Li, S. Wu, B. Zhang, S. Zhang, C. Wang, X. Miao, J. Li, W. Liu, H. Zhang, Clinical Characteristics of 54 medical staff with COVID-19: A retrospective study in a single center in Wuhan, China, Journal of Medical Virology (March) (2020) 1–7, doi:10.1002/jmv.25793.
[9] Coronavirus disease (covid-2019) situation reports, 2020, (https://www.who.int/emergencies/diseases/novel-coronavirus-2019/situation-reports). Accessed: 17.04.20.
[10] L.C. de Castro Medeiros, C.A.R. Castilho, C. Braga, W.V. de Souza, L. Regis, A.M.V. Monteiro, Modeling the dynamic transmission of dengue fever: Investigating disease persistence, PLoS Neglected Tropical Diseases 5 (1) (2011) 1–14, doi:10.1371/journal.pntd.0000942.
[11] O. Diekmann, J.A. Heesterbeek, M.G. Roberts, The construction of next-generation matrices for compartmental epidemic models, Journal of the Royal Society Interface 7 (47) (2010) 873–885, doi:10.1098/rsif.2009.0386.
[12] R.J. Doran, S.W. Laffan, Simulating the spatial dynamics of foot and mouth disease outbreaks in feral pigs and livestock in Queensland, Australia, using a susceptible-infected- recovered cellular automata model, Preventive Veterinary Medicine 70 (1-2) (2005) 133–152, doi:10.1016/j.prevetmed.2005.03.002.
[13] M. Eghtesadi, Breaking Social Isolation Amidst COVID-19: A Viewpoint on Improving Access to Technology in Long-Term Care Facilities, Journal of the American Geriatrics Society (2020) 1–2, doi:10.1111/jgs.16478.
[14] S. Eubank, H. Guclu, V.S. Kumar, M.V. Marathe, A. Srinivasan, Z. Toroczkai, N. Wang, Modelling disease outbreaks in realistic urban social networks, Nature 429 (6988) (2004) 180–184, doi:10.1038/nature02541.
[15] N.M. Ferguson, D. Laydon, G. Nedjati-Gilani, N. Imai, K. Ainslie, M. Baguelin, S. Bhatia, A. Boonyasiri, Z. Cucunubá, G. Cuomo-Dannenburg, A. Dighe, I. Dorigatti, H. Fu, K. Gaythorpe, W. Green, A. Hamlet, W. Hinsley, L.C. Okell, S. Van Elsland, H. Thompson, R. Verity, E. Volz, H. Wang, Y. Wang, P. Gt Walker, C. Walters, P. Winskill, C. Whittaker, C.A. Donnelly, S. Riley, A.C. Ghani, Impact of non-pharmaceutical interventions (NPIs) to reduce COVID-19 mortality and healthcare demand, Faculty of Medicine / School of Public Health / Imperial College London (March) (2020) 3–20, doi:10.25561/77482.
[16] D.F. Ferraz, L.H. Monteiro, The impact of imported cases on the persistence of contagious diseases, Ecological Complexity 40 (July) (2019) 100788, doi:10.1016/j.ecocom.2019.100788.
[17] G. Giordano, F. Blanchini, R. Bruno, P. Colaneri, A. Di Filippo, A. Di Matteo, M. Colaneri, Modelling the COVID-19 epidemic and implementation of population-wide interventions in Italy, Nature, 2020, doi:10.1038/s41591-020-0883-7.
[18] A. Holko, M. Mędrek, Z. Pastuszak, K. Phusavat, Epidemiological modeling with a population density map-based cellular automata simulation system, Expert Systems with Applications 48 (2016) 1–8, doi:10.1016/j.eswa.2015.08.018.
[19] C. Hou, J. Chen, Y. Zhou, L. Hua, J. Yuan, S. He, Y. Guo, S. Zhang, Q. Jia, C. Zhao, J. Zhang, G. Xu, E. Jia, The effectiveness of the quarantine of Wuhan city against the Corona Virus Disease 2019 (COVID-19): well-mixed SEIR model analysis, Journal of Medical Virology 2019 (2020) 0–3, doi:10.1002/jmv.25827.
[20] R. Huang, M. Liu, Y. Ding, Spatial-temporal distribution of COVID-19 in China and its prediction: A data-driven modeling analysis, The Journal of Infection in Developing Countries 14 (03) (2020) 246–253, doi:10.3855/jidc.12585.
[21] K. Iwata, C. Miyakoshi, A Simulation on Potential Secondary Spread of Novel Coronavirus in an Exported Country Using a Stochastic Epidemic SEIR Model, Journal of Clinical Medicine 9 (4) (2020) 944, doi:10.3390/jcm9040944.
[22] N.P. Jewell, J.A. Lewnard, B.L. Jewell, Predictive Mathematical Models of the COVID-19 Pandemic: Underlying Principles and Value of Projections, JAMA (2020), doi:10.1001/jama.2020.6585.
[23] M.J. Keeling, C.A. Gilligan, Bubonic plague: A metapopulation model of a zoonosis, Proceedings of the Royal Society B: Biological Sciences 267 (1458) (2000) 2219–2230, doi:10.1098/rspb.2000.1272.
[24] H.H. Khachfe, M. Chahrour, J. Sammouri, H.A. Salhab, B.E. Makki, M.Y. Fares, An Epidemiological Study on COVID-19: A Rapidly Spreading Disease, Cureus 12 (3) (2020), doi:10.7759/cureus.7313.
[25] M. Ki, Epidemiologic characteristics of early cases with 2019 novel coronavirus (2019-nCoV) disease in Korea, Epidemiology and health 42 (2020) e2020007, doi:10.4178/epih.e2020007.
[26] A. Lachmann, K.M. Jagodnik, F.M. Giorgi, F. Ray, Correcting under-reported COVID-19 case numbers: estimating the true scale of the pandemic, medRxiv (2020), doi:10.1101/2020.03.14.20036178. 2020.03.14.20036178
[27] K. Leung, J.T. Wu, D. Liu, G.M. Leung, Articles First-wave COVID-19 transmissibility and severity in China outside Hubei after control measures, and second-wave scenario planning : a modelling impact assessment, The Lancet 6736 (20) (2020), doi:10.1016/S0140-6736(20)30746-7.
[28] W. Lyra, J.D. do Nascimento, J. Belkhiria, L. de Almeida, P.P.M. Chrispim, I. de Andrade, COVID-19 pandemics modeling with modified determinist SEIR, social distancing, and age stratification. The effect of vertical confinement and release in Brazil, PLoS ONE 15 (9) (2020) 1–17, doi:10.1371/journal.pone.0237627.
[29] Mapa brasileiro da covid-19, 2020, (https://mapabrasileirodacovid.inloco.com.br/). Accessed: 11.05.20.
[30] M.E. Marziali, K.G. Card, T. McLinden, L. Wang, J. Trigg, R.S. Hogg, Physical Distancing in COVID-19 May Exacerbate Experiences of Social Isolation among People Living with HIV, AIDS and Behavior (1) (2020) 8–10, doi:10.1007/s10461-020-02872-8.
[31] Ministério da saúde - covid-19, 2020. (https://coronavirus.saude.gov.br/). Accessed: 15.04.20
[32] L.H.A. Monteiro, H.D.B. Chimara, J.G.C. Berlinck, Big cities : Shelters for contagious diseases, Ecological Modelling 197 (2006) 258–262, doi:10.1016/j.ecolmodel.2006.02.042.
[33] J. Mossong, N. Hens, M. Jit, P. Beutels, K. Auranen, R. Mikolajczyk, M. Massari, S. Salmaso, G.S. Tomba, J. Wallinga, J. Heijne, M. Sadkowska-Todys, M. Rosinska, W.J. Edmunds, Social contacts and mixing patterns relevant to the spread of infectious diseases, PLoS Medicine 5 (3) (2008) 0381–0391, doi:10.1371/journal.pmed.0050074.
[34] F.M. Pereira, P.H. Schimit, Dengue fever spreading based on probabilistic cellular automata with two lattices, Physica A: Statistical Mechanics and its Applications 499 (2018) 75–87, doi:10.1016/j.physa.2018.01.029.
[35] P. Pongsumpun, D.G. Lopez, C. Favier, L. Torres, J. Llosa, M.A. Dubois, Dynamics of dengue epidemics in urban contexts, 2008, 10.1111/j.1365-3156.2008.02124.x
[36] Projeções e estimativas da população do brasil e das unidades da federação, 2020, (https://www.ibge.gov.br/apps/populacao/projecao/). Accessed: 24.04.20.
[37] A.B. Ramos, P.H. Schimit, Disease spreading on populations structured by groups, Applied Mathematics and Computation 353 (2019) 265–273, doi:10.1016/j.amc.2019.01.055.
[38] Recursos físicos - hospitalar - leitos de internação - brasil, tabnet, datasus, (http://tabnet.datasus.gov.br/cgi/tabcgi.exe?cnes/cnv/leiintbr.def). Accessed: 15.04.20.
[39] W.C. Roda, M.B. Varughese, D. Han, M.Y. Li, Why is it difficult to accurately predict the COVID-19 epidemic? Infectious Disease Modelling 5 (2020) 271–281, doi:10.1016/j.idm.2020.03.001.
[40] X. Rong, L. Yang, H. Chu, M. Fan, Effect of delay in diagnosis on transmission of COVID-19, Mathematical Biosciences and Engineering 17 (3) (2020) 2725–2740, doi:10.3934/mbe.2020149.
[41] P. Schimit, F. Pereira, Disease spreading in complex networks: A numerical study with Principal Component Analysis, Expert Systems with Applications 97 (2018), doi:10.1016/j.eswa.2017.12.021.
[42] P.H.T. Schimit, L.H.A. Monteiro, On the basic reproduction number and the topological properties of the contact network: An epidemiological study in mainly locally connected cellular automata, Ecological Modelling 220 (7) (2009) 1034–1042.
[43] P.H.T. Schimit, L.H.A. Monteiro, A vaccination game based on public health actions and personal decisions, Ecological Modelling 222 (9) (2011) 1651–1655, doi:10.1016/j.ecolmodel.2011.02.019.
[44] N. Sharma, A.K. Gupta, Impact of time delay on the dynamics of SEIR epidemic model using cellular automata, Physica A: Statistical Mechanics and its Applications 471 (2017) 114–125, doi:10.1016/j.physa.2016.12.010.
[45] G.C. Sirakoulis, I. Karafyllidis, A. Thanailakis, A cellular automaton model for the effects of population movement and vaccination on epidemic propagation, Ecological Modelling 133 (3) (2000) 209–223.
[46] R. Slimi, S. El Yacoubi, E. Dumonteil, S. Gourbière, A cellular automata model for Chagas disease, Applied Mathematical Modelling 33 (2) (2009) 1072–1085, doi:10.1016/j.apm.2007.12.028.
[47] P. Song, T. Karako, COVID-19: Real-time dissemination of scientific information to fight a public health emergency of international concern, BioScience Trends 14 (1) (2020) 1–2, doi:10.5582/BST.2020.01056.
[48] J.H. Tanne, E. Hayasaki, M. Zastrow, P. Pulla, P. Smith, A.G. Rada, Covid-19: How doctors and healthcare systems are tackling coronavirus worldwide, The BMJ 368 (March) (2020) 1–5, doi:10.1136/bmj.m1090.
[49] Taxa de ocupação geral, (http://tabnet.datasus.gov.br/cgi/tabcgi.exe?cnes/cnv/leiintbr.def). Accessed: 15.04.20.
[50] Tábuas completas de mortalidade, 2020. (https://www.ibge.gov.br/estatisticas/sociais/populacao/9126-tabuas-completas-de-mortalidade.html). Accessed: 15.04.20
[51] F. Verelst, E. Kuylen, P. Beutels, Indications for healthcare surge capacity in European countries facing an exponential increase in coronavirus disease (COVID-19) cases, March 2020, Eurosurveillance 25 (13) (2020) 1–4, doi:10.2807/1560-7917.es.2020.25.13.2000323.
[52] R. Verity, L.C. Okell, I. Dorigatti, P. Winskill, C. Whittaker, N. Imai, G. Cuomo-Dannenburg, H. Thompson, P. Walker, H. Fu, A. Dighe, J. Griffin, A. Cori, M. Baguelin, S. Bhatia, A. Boonyasiri, Z.M. Cucunuba, R. Fitzjohn, K.A.M. Gaythorpe, W. Green, A. Hamlet, W. Hinsley, D. Laydon, G. Nedjati-Gilani, S. Riley, S. Van-Elsand, E. Volz, H. Wang, Y. Wang, X. Xi, C. Donnelly,

A. Ghani, N. Ferguson, Estimates of the severity of COVID-19 disease, medRxiv (2020), doi:10.1101/2020.03.09.20033357. 2020.03.09.20033357

[53] K. Wan, J. Chen, C. Lu, L. Dong, Z. Wu, L. Zhang, When will the battle against novel coronavirus end in Wuhan: A SEIR modeling analysis, Journal of Global Health 10 (1) (2020), doi:10.7189/jogh.10.011002.

[54] R. Wölfel, V.M. Corman, W. Guggemos, M. Seilmaier, S. Zange, M.A. Müller, D. Niemeyer, T.C. Jones, P. Vollmar, C. Rothe, M. Hoelscher, T. Bleicker, S. Brünink, J. Schneider, R. Ehmann, K. Zwirglmaier, C. Drosten, C. Wendtner, Virological assessment of hospitalized patients with COVID-2019, Nature (2020) 1–10, doi:10.1038/s41586-020-2196-x.

[55] Worldometer. Coronavirus, 2020, (https://www.worldometers.info/coronavirus/). Accessed: 12.05.20.

[56] H. Xiao, Y. Zhang, D. Kong, S. Li, N. Yang, The Effects of Social Support on Sleep Quality of Medical Staff Treating Patients with Coronavirus Disease 2019 (COVID-19) in January and February 2020 in China, Medical science monitor : international medical journal of experimental and clinical research 26 (2020) e923549, doi:10.12659/MSM.923549.

[57] X. Xiao, S.H. Shao, K.C. Chou, A probability cellular automaton model for hepatitis B viral infections, Biochemical and Biophysical Research Communications 342 (2) (2006) 605–610, doi:10.1016/j.bbrc.2006.01.166.

[58] S. Xu, Y. Li, Beware of the second wave of COVID-19., Lancet (London, England) 2019 (20) (2020) 2019–2020, doi:10.1016/S0140-6736(20)30845-X.

[59] S. Yakowitz, J. Gani, R. Hayes, Cellular automaton modeling of epidemics, Appl. Math. Comp. 40 (1990) 41–54.

[60] W. Yang, Q. Cao, L. Qin, X. Wang, Z. Cheng, A. Pan, J. Dai, Q. Sun, F. Zhao, J. Qu, F. Yan, Clinical characteristics and imaging manifestations of the 2019 novel coronavirus disease (COVID-19):A multi-center study in Wenzhou city, Zhejiang, China, Journal of Infection 80 (4) (2020) 388–393, doi:10.1016/j.jinf.2020.02.016.

[61] Z. Yang, Z. Zeng, K. Wang, S.-S. Wong, W. Liang, M. Zanin, P. Liu, X. Cao, Z. Gao, Z. Mai, J. Liang, X. Liu, S. Li, Y. Li, F. Ye, W. Guan, Y. Yang, F. Li, S. Luo, Y. Xie, B. Liu, Z. Wang, S. Zhang, Y. Wang, N. Zhong, J. He, Modified SEIR and AI prediction of the epidemics trend of COVID-19 in China under public health interventions, Journal of Thoracic Disease 12 (3) (2020) 165–174, doi:10.21037/jtd.2020.02.64.

[62] P. Yu, J. Zhu, Z. Zhang, Y. Han, A Familial Cluster of Infection Associated With the 2019 Novel Coronavirus Indicating Possible Person-to-Person Transmission During the Incubation Period, The Journal of Infectious Diseases (2020) 1–5, doi:10.1093/infdis/jiaa077. Xx Xxxx